

The role of the subtropical jet in deficient winter precipitation across the mid-Holocene Indus basin

Article

Accepted Version

Hunt, K. M. R. and Turner, A. G. (2019) The role of the subtropical jet in deficient winter precipitation across the mid-Holocene Indus basin. *Geophysical Research Letters*, 46 (10). pp. 5452-5459. ISSN 0094-8276 doi: <https://doi.org/10.1029/2019GL081920> Available at <http://centaur.reading.ac.uk/83142/>

It is advisable to refer to the publisher's version if you intend to cite from the work. See [Guidance on citing](#).

To link to this article DOI: <http://dx.doi.org/10.1029/2019GL081920>

Publisher: American Geophysical Union

All outputs in CentAUR are protected by Intellectual Property Rights law, including copyright law. Copyright and IPR is retained by the creators or other copyright holders. Terms and conditions for use of this material are defined in

the [End User Agreement](#).

www.reading.ac.uk/centaur

CentAUR

Central Archive at the University of Reading

Reading's research outputs online

1 **The role of the subtropical jet in deficient winter**
2 **precipitation across the mid-Holocene Indus basin**

3 **K. M. R. Hunt^{1,2}, A. G. Turner^{1,2}**

4 ¹Department of Meteorology, University of Reading, United Kingdom

5 ²National Centre for Atmospheric Science, University of Reading, United Kingdom

6 **Key Points:**

- 7 • Greater seasonality during the mid-Holocene reduces temperature gradient and
8 weakens the subtropical jet in northern hemisphere winter. (135 chars)
- 9 • Weaker and less frequent western disturbances reach South Asia, leading to a 15%
10 fall in winter precipitation in the Indus Basin. (129 chars)
- 11 • The known stronger summer monsoon combined with reduced winter rainfall gives
12 a striking shift in seasonality in the mid-Holocene. (130 chars)

Corresponding author: Kieran M. R. Hunt, k.m.r.hunt@reading.ac.uk

Abstract

The mid-Holocene (7-5 ka) was a period with an increased seasonal insolation cycle, resulting from decreased insolation during northern hemisphere winter. Here, a set of six CMIP5 models is used to show that the decreased insolation reduced the upper-tropospheric meridional temperature gradient, producing a weaker subtropical jet with less horizontal shear.

These effects work to reduce the baroclinic and barotropic instability available for perturbations to grow, and in consequence, storm-tracking results show that there are fewer winter storms over India and Pakistan (known as western disturbances). These western disturbances are weaker, resulting in a reduction in winter precipitation of around 15% in the north Indus Basin.

Combined with previous work showing greater northwestward extent of the Indian monsoon during the mid-Holocene, our GCM-derived results are consistent with the Indus Basin changing from a summer-growing season in the mid-Holocene to a winter-growing season in the present day.

1 Introduction

The subtropical westerly jet (STWJ) is a quasi-permanent feature of the Eurasian upper troposphere (Krishnamurti, 1961), a thermal wind brought about by a strong meridional temperature gradient. It exhibits a distinctive seasonal cycle in latitude: at Indian longitudes during the boreal summer, it is at approximately 25°N, moving north of the Tibetan Plateau during the monsoon to about 45°N (Schiemann, Lüthi, & Schär, 2009). Embedded within the STWJ are numerous eddies, which intensify in the baroclinically unstable environment on approach to India and Pakistan (Hunt, Curio, Turner, & Schiemann, 2018), where they become known as western disturbances (WDs). WDs are responsible for a large majority of winter rainfall in Pakistan and north India (Hunt, Turner, & Shaffrey, 2019; Martyn, 2002; Syed, Giorgi, Pal, & King, 2006), a region thoroughly dependent on winter agriculture.

The mid-Holocene (\sim 7-5 ka; taken as 6 ka for simulations) is the name given to the warm period that occurred during the middle of the current interglacial; orbital precession, with minor contributions from increased orbital obliquity and eccentricity resulted in a stronger seasonal cycle and a shallower meridional temperature gradient (e.g. Bosmans

44 et al., 2012; Harrison et al., 2003). As a result, both proxies and climate models suggest
45 that the South Asian monsoon had a greater magnitude and deeper northwestward ex-
46 tent during this period (Braconnot et al., 2002, 2007; Bryson & Swain, 1981; Joussaume
47 et al., 1999; Liu, Harrison, Kutzbach, & Otto-Bliesner, 2004; Rawat, Gupta, Srivastava,
48 Sangode, & Nainwal, 2015).

49 The end of the mid-Holocene (MH) period marked the economic and social collapse
50 of a large civilisation in the Indus basin, the so-called Harappan Civilisation (Misra, 1984;
51 Possehl, 1997a, 1997b). Authors have attributed this to variety of possibly connected
52 causes: the drying up of important Indus tributaries (e.g. Dikshit, 1979), rerouting of
53 tributaries (Raikes & Dales, 1986), changing flood hazards (Flam, 2002), and changing
54 seasonality of the river discharge available for irrigation (Giosan et al., 2012). These are
55 typically attributed to the contemporaneous and permanent withdrawal of the summer
56 monsoon from the region (Berkelhammer et al., 2012; Staubwasser, Sirocko, Grootes, &
57 Segl, 2003), as described above.

58 Even so, reviewing authors have long argued the need to consider the changes in
59 annual precipitation to the region (Bryson & Swain, 1981; Pant & Maliekal, 1987; Raikes
60 & Dyson, 1961) given the significant contribution of WDs to the present-day climate.
61 Bryson (1997) noted, however, that winter rainfall proxies for the region (e.g. Bryson,
62 1992) are not only sparse but, when used to assess the difference between mid-Holocene
63 and present day precipitation, fail to agree in sign let alone magnitude and pointed out
64 the need for further research on the topic, which thus far has not been conclusive (Madella
65 & Fuller, 2006). Recent isotopic modelling work (J. Li et al., 2017) indicated that pre-
66 cipitation proxies did not agree in the nearby Tibetan Plateau.

67 Nevertheless, this region is capable of trends of measurable magnitude, as seen in
68 recent observations (You et al., 2017). Palazzi, Hardenberg, and Provenzale (2013); Palazzi,
69 von Hardenberg, Terzago, and Provenzale (2015) showed that in both present-day CMIP5
70 experiments and observations, the seasonal cycle shifts from summer-dominated (mon-
71 soonal) precipitation in the central and eastern Himalaya to winter-dominated (western
72 disturbance) precipitation in the western Himalaya and Karakoram. Thus, if the sum-
73 mer monsoon had a more westward extent during the mid-Holocene, we would expect
74 important changes to the seasonal cycle in this region.

75 So, previous studies have established that the summer monsoon extended further
76 into the Indus basin during the mid-Holocene, and that this is a region that contains a
77 transition in the seasonal cycle of precipitation. It is not clear, however, what happened
78 to the boreal winter STWJ during the mid-Holocene – and thus how western disturbances
79 were affected; though some authors (Hou, D’Andrea, Wang, He, & Liang, 2017; Wei &
80 Wang, 2004) have noted that the summer STWJ was climatologically further north in
81 the mid-Holocene. Here, we seek to quantify and understand how the jet behaves in CMIP5
82 simulations of the mid-Holocene, before using a tracking algorithm to identify changes
83 in western disturbance populations between the mid-Holocene and present-day climates
84 for the first time; we will then finish by exploring how these changes play a role in the
85 seasonality of precipitation over the Indus basin and Karakoram.

86 2 Data

87 In this study, we make use of outputs from six CMIP5 models - that is all those
88 that have six-hourly output for winds in both the mid-Holocene and historical experi-
89 ments. These experiments comprise a subset of the Paleoclimate Model Intercompar-
90 ison Project (PMIP3; Braconnot et al., 2012). Details of those models are given in Tab. 1.
91 Where data availability permits, the table also gives the value of the winter (DJFM) west-
92 ern disturbance frequency bias – indicating whether the historical climatology (1950-2005)
93 of the model produces too many or too few WDs compared to ERA-Interim (which has
94 about 25 per winter, using our tracking algorithm). The models used in this study com-
95 prise a fairly representative spread of biases (the multi-model mean bias for all CMIP5
96 historical models is about +13%, see Hunt et al., 2019), which is important given the
97 resolution sensitivity of WD behaviour in climate models. When combined to assess multi-
98 model means, data are interpolated onto a common, coarse grid.

103 We use the western disturbance tracking algorithm described in Hunt, Turner, and
104 Shaffrey (2018), tuned for use in CMIP5 GCMs by Hunt et al. (2019). The six-hourly
105 relative vorticity is spectrally truncated at T63 to remove orographic noise and mesoscale
106 eddies, and to provide a common grid between the model outputs. Maxima at 500 hPa
107 are identified and connected using a $k-d$ tree nearest neighbour algorithm (Yianilos,
108 1993) to form tracks, subject to constraints on propagation speed, track smoothness, and
109 track duration (systems shorter than two days are considered transient). Finally, tracks
110 that are shorter than 48 hours in duration or do not pass eastward through the box 20°N-

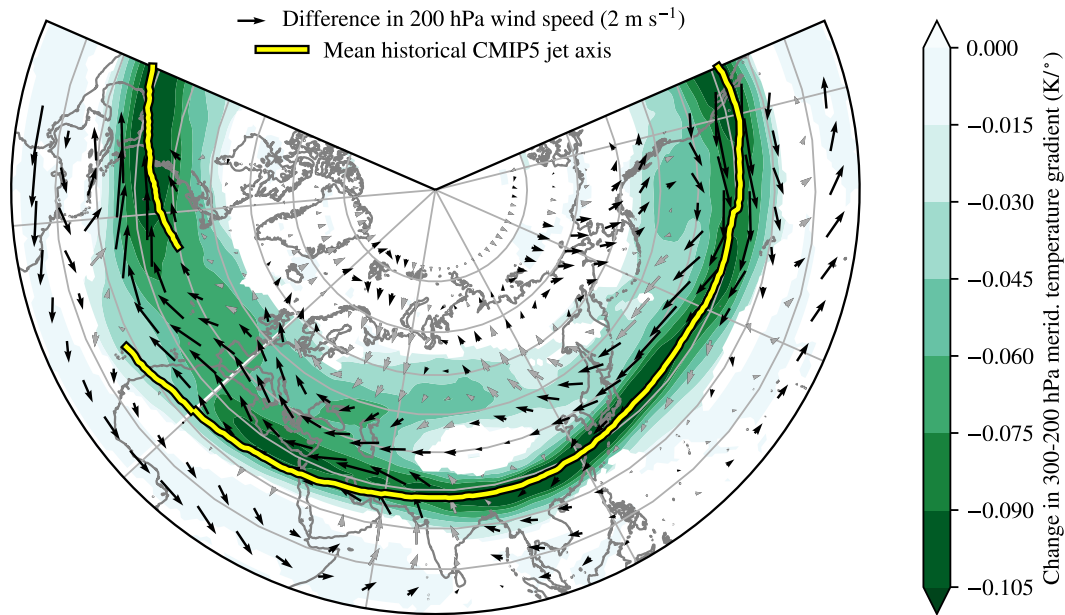
Model name	Organisation	$n_x \times n_y$	$\delta_x \times \delta_y$	WWD freq. bias	Reference
bcc-csm1-1*	BCC	128×64	2.81° × 2.79°	+38%	Wu et al. (2013)
CCSM4	NCAR	288×191	1.25° × 0.94°	n/a	Meehl et al. (2012)
CNRM-CM5	CNRM-CERFACS	256×128	1.41° × 1.40°	n/a	Voldoire et al. (2013)
CSIRO-Mk3-6-0*	CSIRO-QCCCE	192×96	1.88° × 1.87°	+44%	Rotstayn et al. (2010)
FGOALS-g2*	LASG-CESS	128×64	2.81° × 2.79°	+4%	L.-J. Li et al. (2013)
FGOALS-s2	LASG-CESS	128×108	2.81° × 1.66°	n/a	L.-J. Li et al. (2013)
GISS-E2-R	NASA-GISS	144×90	2.5° × 2°	n/a	Schmidt et al. (2006)
HadGEM2-CC*	MOHC	192×144	1.88° × 1.25°	+22%	Martin et al. (2011)
HadGEM2-ES	MOHC	192×144	1.88° × 1.25°	n/a	Martin et al. (2011)
IPSL-CM5a-LR*	IPSL	96×95	3.75° × 1.89°	-25%	Dufresne et al. (2013)
MPI-ESM-P*	MPI-M	192×96	1.88° × 1.87°	+35%	Giorgetta et al. (2013)

99 **Table 1.** Details of the eleven CMIP5 models used in this study, those marked with an aster-
100 isk have six-hourly output and are thus the ones used for tracking. Where available, the bias in
101 winter (DJFM) western disturbance frequency in the model (computed against ERA-Interim) is
102 given.

111 36.5°N, 60°E-80°E are discarded. Using this domain ensures tracks pass through Pak-
112 istan and/or north India and filters out mid-tropospheric cyclones, which are a tropi-
113 cal phenomenon that would otherwise satisfy the tracking criteria. Output tracks are ver-
114 ified against previous case studies to check completeness, and subsequent structure and
115 cluster analysis shows that no secondary systems contaminate the database. The inter-
116 ested reader is encouraged to visit Sec 2.2 of Hunt, Turner, and Shaffrey (2018) for a de-
117 tailed description of the algorithm.

118 3 Results

126 We start by exploring how changes to the upper-tropospheric meridional temper-
127 ature gradient (UTTG) affect the winter STWJ in mid-Holocene experiments. Fig. 1 shows
128 the change in UTTG between the mid-Holocene and present day, as well as the change
129 in 200 hPa winds, and for illustration the mean location of the STWJ in CMIP5 present-
130 day runs. For consistency throughout, we use the convention that ‘change’ refers exactly
131 to mid-Holocene minus present day (or control). Here, we choose the UTTG to be pos-

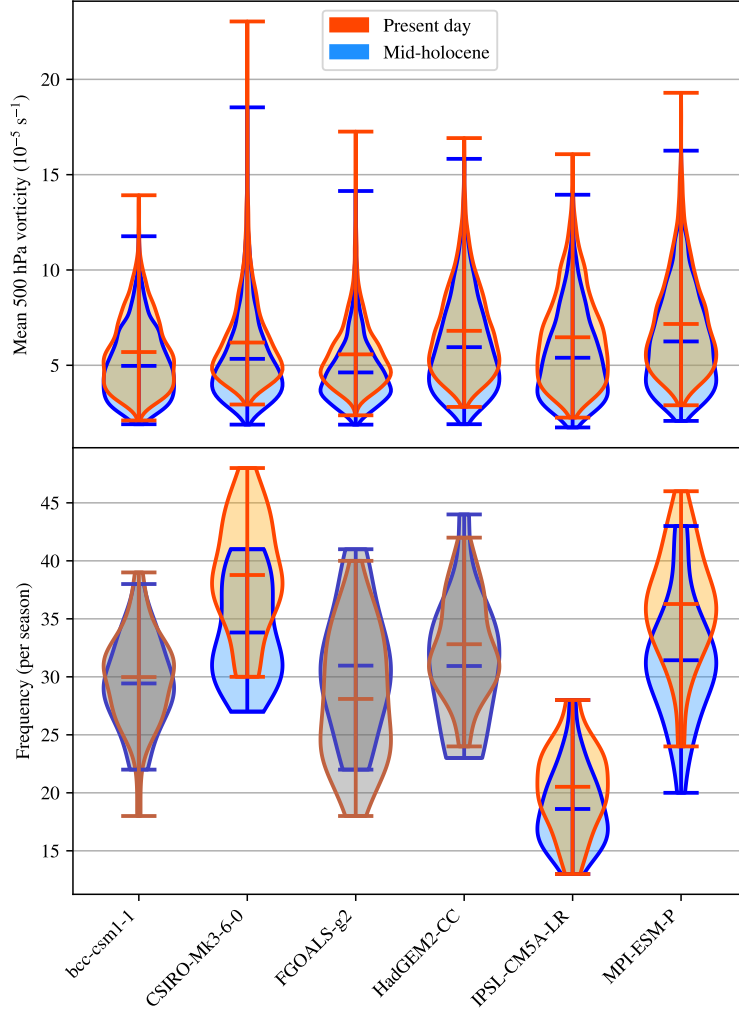


119 **Figure 1.** The change (i.e. mid-Holocene minus present day) in DJFM upper level meridional
 120 T gradient [$\text{K}/^\circ$], defined as positive when temperature increases in the equatorward direction.
 121 Overlaid in quivers are the associated 200 hPa circulation differences, showing retardation and
 122 reduced shear of the jet in the MH. Both are computed for the six models in which WD tracking
 123 was performed; quivers are grey and contours masked where any model disagrees on the sign
 124 of change in zonal wind or temperature gradient change respectively. For reference, the mean
 125 present-day CMIP5 jet axis is also shown.

132 itive (i.e. pole-to-equator gradient, rather than equator to pole), thus the more negative
 133 the value is in Fig. 1, the weaker the gradient in the mid-Holocene when compared to
 134 present-day.

135 We see that the expected decline of the UTTG correlates strongly with a weaken-
 136 ing of the winter STWJ, particularly along its northern flank. There are two important
 137 corollaries: firstly, the smaller temperature gradient, particularly upstream of India, im-
 138 plies that there is less baroclinic instability from which perturbations in the jet can feed
 139 off; secondly, the reduction in STWJ strength implies the same for barotropic growth
 140 (the relationship between the STWJ and instabilities is discussed in greater detail in Hunt,
 141 Curio, et al., 2018).

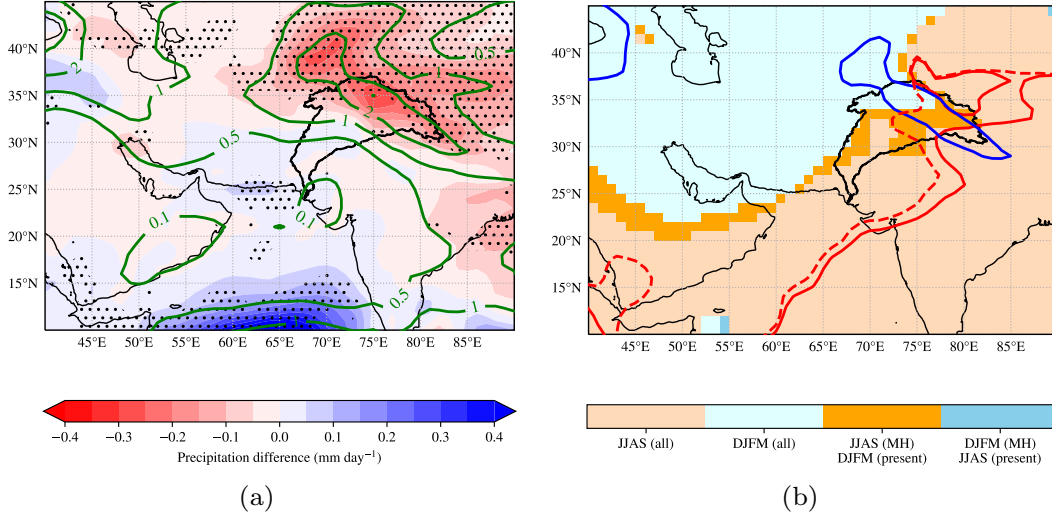
147 We hypothesise, therefore, that WDs incident on India during mid-Holocene win-
 148 ters would be weaker and - perhaps - less frequent than the present day. To test this,



142 **Figure 2.** Violin plots indicating the distributions in (top) the seasonal mean western dis-
 143 turbance 500 hPa vorticity and (bottom) the seasonal frequency of DJFM western disturbances
 144 for (blue) the mid-Holocene and (orange) the present day, by model. Horizontal lines demarcate
 145 minima, means, and maxima respectively. Where the two distributions for a given model are not
 146 significantly different from each other, they are greyed out.

149 an objective tracking algorithm was applied to the six CMIP5/PMIP3 models that had
 150 mid-Holocene experiments with six-hourly output (see Table 1), and their present-day
 151 counterparts. Statistics for WD frequency and intensity are given for each experiment
 152 in Fig. 2, with mid-Holocene in blue and present-day in orange. All experiments record
 153 a statistically significant reduction in intensity (defined as the maximum 500 hPa rel-
 154 ative vorticity attained between 60°E and 80°E), with the multi-model mean difference
 155 amounting to $\sim 17\%$; three also record a statistically significant decline in seasonal fre-

156 quency, with a multi-model mean difference of $\sim 7\%$ across all six models. Three mod-
 157 els do not exhibit a significant change in frequency: bcc-csm1-1, FGOALS-g2, and HadGEM2-
 158 CC. Note that the 500 hPa level is chosen as it is the CMIP5 output level closest to the
 159 observed centre of WDs (~ 400 hPa), and that all frequency and intensity analysis is
 160 done within the described domain ($20\text{-}36.5^\circ\text{N}$, $60\text{-}80^\circ\text{E}$).

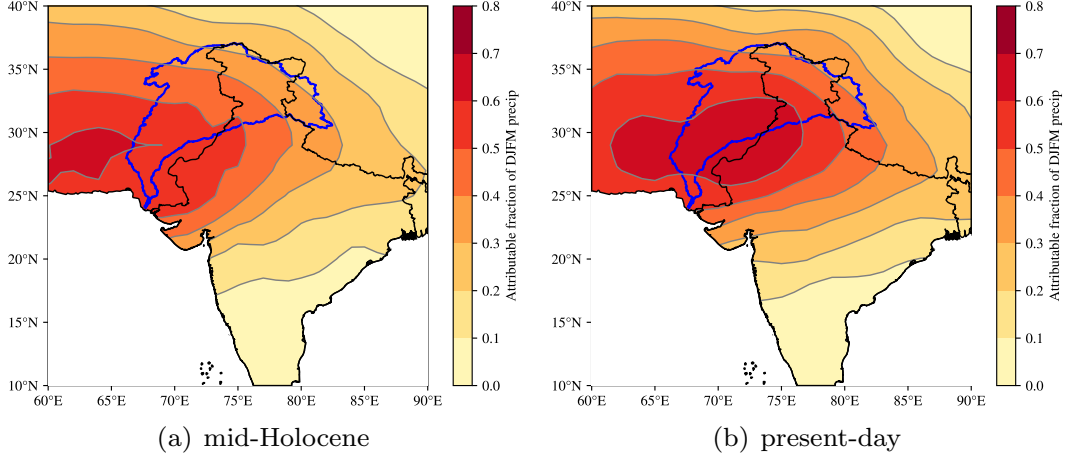


161 **Figure 3.** (a) CMIP5 MMM DJFM precipitation [lines, mm day^{-1}] for the historical exper-
 162 iments (in those six models with a mid-Holocene counterpart with six-hourly output) and the
 163 difference between mid-Holocene and historical MMM DJFM precipitation [solid, mm day^{-1}].
 164 Stippling indicates where all six models agree on the sign of the change. (b) Season of greatest
 165 precipitation: light yellow and light teal indicate regions where the season is the same for both
 166 MH and historical MMMs (JJAS and DJFM respectively), whereas the dark colours indicate that
 167 the seasonality changes (i.e. dark yellow indicates an area where MH precipitation is greatest in
 168 JJAS, but historical precipitation peaks in DJFM, and vice versa for dark teal); historical MMM
 169 2 mm day^{-1} isohyets are given for DJFM and JJAS by the dark blue and red lines respectively
 170 with mid-Holocene JJAS in dashed red. In both figures, the Indus river basin is marked in solid
 171 black.

172 We have seen that the reduced magnitude of the UTTG in the mid-Holocene both
 173 directly (through baroclinic instability of the gradient) and indirectly (through weak-
 174 ening of the STWJ) reduces the frequency and intensity of winter WDs over Pakistan
 175 and north India. As previous studies (e.g. Hunt et al., 2019) have indicated, WDs are
 176 responsible for almost all winter precipitation in Pakistan, north India, and along much

177 of the Himalayan foothills; so how is mid-Holocene winter precipitation in this region af-
178 fected by their weakening?

179 Fig. 3(a) shows the CMIP5 MMM DJFM precipitation climatology (for those mod-
180 els with a MH counterpart experiment), and the change between the MH and the present
181 day. At the head of the Indus basin, where the precipitation is typically the greatest, the
182 mid-Holocene climatology is between 15 and 20% lower than it is in the present day. Tran-
183 sient simulations have shown that the South Asian summer monsoon was both stronger
184 and had greater extent during the mid-Holocene period (Liu et al., 2004), which agrees
185 with pollen records where available (Lézine, Ivory, Braconnot, & Marti, 2017). Fig. 3(b)
186 compares the winter (DJFM) and summer (JJAS) climatologies for both the historical
187 and mid-Holocene period, indicating the regions in which both or neither dominate the
188 seasonal cycle. The dividing line between winter-dominant (i.e., DJFM) and summer-
189 dominant (i.e., JJAS) precipitation regions retreats southeastward as the mid-Holocene
190 finishes and the extent of the summer monsoon starts to decline. This effect is exagger-
191 ated considerably along the Karakoram (the mountain range spanning north Pakistan
192 and north India) as the winter precipitation also increases as a result of the previous de-
193 scribed changes in WD activity. Fig. S1 shows how the seasonal cycle of precipitation
194 changes in the basin between the two epochs. Supporting Fig. 3(b), it shows a well de-
195 fined boreal summer peak in the mid-Holocene, which moves to a winter-spring peak in
196 the present day. Fourier decomposition (e.g. Dwyer, Biasutti, & Sobel, 2012) reveals that
197 the two cycles have significantly different phase and amplitude. The result from the point
198 of view of the Indus basin is thus twofold: a shift of primary growing season from sum-
199 mer (in the mid-Holocene, e.g. Dave, Courty, Fitzsimmons, & Singhvi, 2018; Giosan et
200 al., 2012) to winter (in the present day, Kalra et al., 2008; Sarker & Quaddus, 2002); and
201 a shift in the location of the area of peak precipitation, from the east and northeast of
202 the basin to the orographic band in the north. Each feature of Fig. 3(a) and Fig. 3(b)
203 discussed in this section persist when the analysis is done with all eleven mid-Holocene
204 models. As discussed in the introduction, there is a dearth of winter/seasonal paleocli-
205 mate reconstructions in the Indus basin; however, a number have looked at proxies in
206 the northwest Himalaya, a region bordering the north/northeast of our domain. Both
207 pollen (Demske, Tarasov, Wünnemann, & Riedel, 2009) and sediment (Prasad & Enzel,
208 2006) records indicate a period of reduced winter precipitation 6 ka before present.



209 **Figure 4.** Fraction of the climatological winter precipitation attributed to western disturbance
 210 activity in (a) mid-Holocene and (b) historical CMIP5 experiments, computed in each case using
 211 the six models for which six-hourly mid-Holocene output is available. Precipitation is attributed
 212 if it occurs within 800 km and 24 hours of a passing WD. The catchment boundary of the Indus
 213 basin is marked in blue.

214 To complete our argument, we must determine whether the change in WDs is re-
 215 sponsible for the change in precipitation. To do that, we can compare the fraction of win-
 216 ter precipitation caused by western disturbances in the mid-Holocene to the present day.
 217 Fig 4 shows that there is a roughly uniform increase of about 0.1 in the fraction of at-
 218 tributed precipitation across the Indus basin from the mid-Holocene to the present-day.
 219 This follows the fractional change seen in Fig. 3(a), and provides strong evidence that
 220 increasing winter rainfall in the region after the mid-Holocene was caused by increased
 221 WD activity.

222 4 Discussion

223 In this study, we have explored how changes in orbital parameters between the mid-
 224 Holocene period (MH; 7-5 ka) and the present day affect the boreal winter subtropical
 225 westerly jet and its impacts on storms known as western disturbances (WDs) which af-
 226 fect northern India and Pakistan. Orbital precession resulted in a more pronounced global
 227 seasonal cycle and acted to reduce the upper-tropospheric meridional temperature gra-
 228 dient in boreal winter. We have shown that this reduction in gradient weakens the north-
 229 ern flank of the subtropical westerly jet, which previous studies (Hunt, Curio, et al., 2018)

230 have shown result in less baroclinic and barotropic instability for WDs when they reach
231 India - to feed off. This resulted in mid-Holocene South Asia being impacted by weaker
232 and less frequent WDs. All six models used in this study agreed that WD intensity was
233 significantly lower during the mid-Holocene, though a significant decline in WD frequency
234 was found in only three.

235 Since WDs are very strongly tied to winter rainfall over Pakistan and northern In-
236 dia (where they are typically responsible for about 70% of present day winter precipi-
237 tation), the reduced activity during the mid-Holocene resulted in a decline of about 15%
238 in winter precipitation at the head of the Indus basin. Previous studies have shown that
239 the South Asian summer monsoon was stronger and had a greater northwestward ex-
240 tent during the mid-Holocene; combined with the previous result, this has a profound
241 impact on the Indus river basin. There, in the mid-Holocene, most precipitation fell dur-
242 ing the summer monsoon, focused in the east; instead in the present day, most precip-
243 itation falls during the winter, and tends to be focused in the north, along the orogra-
244 phy.

245 This change in growing season is complementary to previous explanations for the
246 collapse of the Harappan Civilisation, which underwent agricultural failure and eastward
247 migration towards the end of the mid-Holocene period. We hope that further work, in
248 particular the discovery of robust proxies for winter precipitation in the region, will con-
249 tinue to explore this problem in more detail.

250 **Acknowledgments**

251 This study was supported by the JPI-Climate and Belmont Forum Climate Predictabil-
252 ity and Inter-Regional Linkages Collaborative Research Action via NERC grant NE/P006795/1.
253 We acknowledge the World Climate Research Programme's Working Group on Coupled
254 Modelling, which is responsible for CMIP (<http://pcmdi9.lln1.gov>), and we thank the
255 climate modeling groups for producing and making available their model output. For CMIP
256 the U.S. Department of Energy's Program for Climate Model Diagnosis and Intercom-
257 parison provides coordinating support and led development of software infrastructure
258 in partnership with the Global Organization for Earth System Science Portals. ERA-
259 Interim reanalysis data are available from ECMWF at [https://www.ecmwf.int/en/forecasts/
260 datasets/reanalysis-datasets/era-interim](https://www.ecmwf.int/en/forecasts/datasets/reanalysis-datasets/era-interim). The tracking algorithm used is avail-

261 able from the first author. Track datasets for ERA-Interim and CMIP5 experiments are
262 available from the BADC at <https://catalogue.ceda.ac.uk/uuid/b1f266c25cf2445f8b87d874f6ac830a>.

263 The authors wish to thank three anonymous reviewers for constructive comments
264 on our manuscript.

265 References

- 266 Berkelhammer, M., Sinha, A., Stott, L., Cheng, H., Pausata, F. S., Yoshimura, K.,
267 et al. (2012). An abrupt shift in the Indian monsoon 4000 years ago. *Geophys.*
268 *Monogr. Ser.*, 198(7).
- 269 Bosmans, J. H. C., Drijfhout, S. S., Tuenter, E., Lourens, L. J., Hilgen, F. J., & We-
270 ber, S. L. (2012). Monsoonal response to mid-holocene orbital forcing in a high
271 resolution gcm. *Climate of the Past*, 8(2), 723–740.
- 272 Braconnot, P., Harrison, S. P., Kageyama, M., Bartlein, P. J., Masson-Delmotte,
273 V., Abe-Ouchi, A., . . . Zhao, Y. (2012). Evaluation of climate models using
274 palaeoclimatic data. *Nature Climate Change*, 2(6), 417.
- 275 Braconnot, P., Loutre, M., Dong, B., Joussaume, S., Valdes, P., et al. (2002). How
276 the simulated change in monsoon at 6 ka BP is related to the simulation of
277 the modern climate: results from the Paleoclimate Modeling Intercomparison
278 Project. *Climate Dynamics*, 19(2), 107–121.
- 279 Braconnot, P., Otto-Bliesner, B., Harrison, S., Joussaume, S., Peterchmitt, J.-Y.,
280 Abe-Ouchi, A., . . . others (2007). Results of PMIP2 coupled simulations of the
281 Mid-Holocene and Last Glacial Maximum—Part 1: experiments and large-scale
282 features. *Climate of the Past*, 3(2), 261–277.
- 283 Bryson, R. A. (1992). A macrophysical model of the holocene intertropical conver-
284 gence and jetstream positions and rainfall for the saharan region. *Meteorology*
285 *and Atmospheric Physics*, 47(2-4), 247–258.
- 286 Bryson, R. A. (1997). Proxy indications of Holocene winter rains in southwest Asia
287 compared with simulated rainfall. In *Third millennium bc climate change and*
288 *old world collapse* (pp. 465–473). Springer.
- 289 Bryson, R. A., & Swain, A. M. (1981). Holocene variations of monsoon rainfall in
290 Rajasthan. *Quaternary Research*, 16(2), 135–145.
- 291 Dave, A. K., Courty, M.-A., Fitzsimmons, K. E., & Singhvi, A. K. (2018). Revisiting
292 the contemporaneity of a mighty river and the Harappans: Archaeological,

- 293 stratigraphic and chronometric constraints. *Quaternary Geochronology*, 49,
294 230–235.
- 295 Demske, D., Tarasov, P. E., Wünnemann, B., & Riedel, F. (2009). Late glacial and
296 holocene vegetation, Indian monsoon and westerly circulation in the Trans-
297 Himalaya recorded in the lacustrine pollen sequence from Tso Kar, Ladakh,
298 NW India. *Palaeogeography, Palaeoclimatology, Palaeoecology*, 279(3), 172–
299 185.
- 300 Dikshit, K. N. (1979). Old channels of Ghaggar in Rajasthan-revisited. *Man and*
301 *Environment*, 3, 105–106.
- 302 Dufresne, J.-L., Foujols, M.-A., Denvil, S., Caubel, A., Marti, O., Aumont, O., ...
303 others (2013). Climate change projections using the IPSL-CM5 Earth System
304 Model: from CMIP3 to CMIP5. *Climate Dynamics*, 40(9-10), 2123–2165.
- 305 Dwyer, J. G., Biasutti, M., & Sobel, A. H. (2012). Projected changes in the seasonal
306 cycle of surface temperature. *Journal of Climate*, 25(18), 6359–6374.
- 307 Flam, L. (2002). Fluvial geomorphology of the lower Indus basin (Sindh, Pakistan)
308 and the Indus civilization. In *Himalaya to the sea* (pp. 186–200). Routledge.
- 309 Giorgetta, M. A., Jungclaus, J., Reick, C. H., Legutke, S., Bader, J., Böttinger, M.,
310 ... others (2013). Climate and carbon cycle changes from 1850 to 2100 in
311 MPI-ESM simulations for the Coupled Model Intercomparison Project phase 5.
312 *Journal of Advances in Modeling Earth Systems*, 5(3), 572–597.
- 313 Giosan, L., Clift, P. D., Macklin, M. G., Fuller, D. Q., Constantinescu, S., Durcan,
314 J. A., ... others (2012). Fluvial landscapes of the harappan civilization.
315 *Proceedings of the National Academy of Sciences*, 109(26), E1688–E1694.
- 316 Harrison, S. P., Kutzbach, J. E., Liu, Z., Bartlein, P. J., Otto-Bliesner, B., Muhs,
317 D., ... Thompson, R. S. (2003). Mid-holocene climates of the Americas:
318 a dynamical response to changed seasonality. *Climate Dynamics*, 20(7-8),
319 663–688.
- 320 Hou, J., D’Andrea, W. J., Wang, M., He, Y., & Liang, J. (2017). Influence of the
321 Indian monsoon and the subtropical jet on climate change on the Tibetan
322 Plateau since the late Pleistocene. *Quaternary Science Reviews*, 163, 84–94.
- 323 Hunt, K. M. R., Curio, J., Turner, A. G., & Schiemann, R. (2018). Subtropi-
324 cal westerly jet influence on occurrence of western disturbances and tibetan
325 plateau vortices. *Geophysical Research Letters*, 45(16), 8629–8636.

- 326 Hunt, K. M. R., Turner, A. G., & Shaffrey, L. C. (2018). The evolution, seasonality,
327 and impacts of western disturbances. *Quart. J. Roy. Meteor. Soc.*, *144*(710),
328 278–290. doi: 10.1002/qj.3200
- 329 Hunt, K. M. R., Turner, A. G., & Shaffrey, L. C. (2019). Representation of western
330 disturbances in CMIP5 models. *J. Climate*. (In press) doi: 10.1175/JCLI-D-18
331 -0420.1
- 332 Joussaume, S., Taylor, K. E., Braconnot, P. J. F. B., Mitchell, J. F. B., Kutzbach,
333 J. E., Harrison, S. P., . . . others (1999). Monsoon changes for 6000 years
334 ago: results of 18 simulations from the Paleoclimate Modeling Intercomparison
335 Project (PMIP). *Geophysical Research Letters*, *26*(7), 859–862.
- 336 Kalra, N., Chakraborty, D., Sharma, A., Rai, H. K., Jolly, M., Chander, S., . . . oth-
337 ers (2008). Effect of increasing temperature on yield of some winter crops in
338 northwest India. *Current Science*, 82–88.
- 339 Krishnamurti, T. N. (1961). The subtropical jet stream of winter. *Journal of Meteo-*
340 *rology*, *18*(2), 172–191.
- 341 Lézine, A.-M., Ivory, S. J., Braconnot, P., & Marti, O. (2017). Timing of the
342 southward retreat of the ITCZ at the end of the Holocene Humid Period in
343 Southern Arabia: Data-model comparison. *Quaternary Science Reviews*, *164*,
344 68–76.
- 345 Li, J., Ehlers, T. A., Werner, M., Mutz, S. G., Steger, C., & Paeth, H. (2017). Late
346 quaternary climate, precipitation $\delta^{18}O$, and indian monsoon variations over the
347 Tibetan Plateau. *Earth and Planetary Science Letters*, *457*, 412–422.
- 348 Li, L.-J., Lin, P.-F., Yu, Y.-Q., Wang, B., Zhou, T.-J., Liu, L., . . . others (2013).
349 The flexible global ocean-atmosphere-land system model, Grid-point Version 2:
350 FGOALS-g2. *Advances in Atmospheric Sciences*, *30*(3), 543–560.
- 351 Liu, Z., Harrison, S. P., Kutzbach, J., & Otto-Bliesner, B. (2004). Global monsoons
352 in the mid-Holocene and oceanic feedback. *Climate Dynamics*, *22*(2-3), 157–
353 182.
- 354 Madella, M., & Fuller, D. Q. (2006). Palaeoecology and the Harappan civilisation of
355 South Asia: a reconsideration. *Quaternary Science Reviews*, *25*(11-12), 1283–
356 1301.
- 357 Martin, G. M., Bellouin, N., Collins, W. J., Culverwell, I. D., Halloran, P. R., Hardi-
358 man, S. C., . . . others (2011). The HadGEM2 family of Met Office Unified

- 359 Model climate configurations. *Geoscientific Model Development*, 4(3), 723–
360 757.
- 361 Martyn, D. (2002). Climates of the world. In *Developments in atmospheric science*
362 (pp. 389–400). Elsevier.
- 363 Meehl, G. A., Washington, W. M., Arblaster, J. M., Hu, A., Teng, H., Tebaldi, C.,
364 ... others (2012). Climate system response to external forcings and climate
365 change projections in CCSM4. *Journal of Climate*, 25(11), 3661–3683.
- 366 Misra, V. N. (1984). Climate, a factor in the rise and fall of the Indus Civilization–
367 Evidence from Rajasthan and beyond. In M. Rangarajan (Ed.), *Environmental*
368 *issues in india, a reader* (pp. 461–490). Pearson.
- 369 Palazzi, E., Hardenberg, J., & Provenzale, A. (2013). Precipitation in the Hindu-
370 Kush Karakoram Himalaya: Observations and future scenarios. *J. Geophys.*
371 *Res. Atmos.*, 118(1), 85–100.
- 372 Palazzi, E., von Hardenberg, J., Terzago, S., & Provenzale, A. (2015). Precipitation
373 in the Karakoram-Himalaya: a CMIP5 view. *Climate Dyn.*, 45(1-2), 21–45.
- 374 Pant, G. B., & Maliekal, J. A. (1987). Holocene climatic changes over northwest In-
375 dia: An appraisal. *Climatic Change*, 10(2), 183–194.
- 376 Possehl, G. L. (1997a). Climate and the eclipse of the ancient cities of the Indus.
377 In *Third millennium bc climate change and old world collapse* (pp. 193–243).
378 Springer.
- 379 Possehl, G. L. (1997b). The transformation of the Indus civilization. *Journal of*
380 *World Prehistory*, 11(4), 425–472.
- 381 Prasad, S., & Enzel, Y. (2006). Holocene paleoclimates of india. *Quaternary Re-*
382 *search*, 66(3), 442–453.
- 383 Raikes, R. L., & Dales, G. F. (1986). Reposte to Wasson’s sedimentological basis of
384 the Mohenjo-Daro flood hypothesis. *Man and Environment*, 10, 33–44.
- 385 Raikes, R. L., & Dyson, R. H. (1961). The prehistoric climate of Baluchistan and
386 the Indus Valley. *American Anthropologist*, 63(2), 265–281.
- 387 Rawat, S., Gupta, A. K., Srivastava, P., Sangode, S., & Nainwal, H. (2015). A
388 13,000 year record of environmental magnetic variations in the lake and peat
389 deposits from the Chandra valley, Lahaul: Implications to Holocene monsoonal
390 variability in the NW Himalaya. *Palaeogeography, palaeoclimatology, palaeoe-*
391 *cology*, 440, 116–127.

- 392 Rotstayn, L. D., Collier, M. A., Dix, M. R., Feng, Y., Gordon, H. B., O’Farrell,
 393 S. P., ... Syktus, J. (2010). Improved simulation of Australian climate and
 394 ENSO-related rainfall variability in a global climate model with an interactive
 395 aerosol treatment. *International Journal of Climatology*, *30*(7), 1067–1088.
- 396 Sarker, R. A., & Quaddus, M. A. (2002). Modelling a nationwide crop planning
 397 problem using a multiple criteria decision making tool. *Computers & Industrial*
 398 *Engineering*, *42*(2-4), 541–553.
- 399 Schiemann, R., Lüthi, D., & Schär, C. (2009). Seasonality and interannual variabil-
 400 ity of the westerly jet in the Tibetan Plateau region. *J. Climate*, *22*(11), 2940–
 401 2957.
- 402 Schmidt, G. A., Ruedy, R., Hansen, J. E., Aleinov, I., Bell, N., Bauer, M., ... others
 403 (2006). Present-day atmospheric simulations using GISS ModelE: Comparison
 404 to in situ, satellite, and reanalysis data. *Journal of Climate*, *19*(2), 153–192.
- 405 Staubwasser, M., Sirocko, F., Grootes, P. M., & Segl, M. (2003). Climate change at
 406 the 4.2 ka BP termination of the Indus valley civilization and Holocene south
 407 Asian monsoon variability. *Geophysical Research Letters*, *30*(8).
- 408 Syed, F. S., Giorgi, F., Pal, J. S., & King, M. P. (2006). Effect of remote forcings on
 409 the winter precipitation of central southwest Asia part 1: observations. *Theo-*
 410 *retical and Applied Climatology*, *86*(1-4), 147–160.
- 411 Voldoire, A., Sanchez-Gomez, E., y Mélia, D. S., Decharme, B., Cassou, C., Sénési,
 412 S., ... others (2013). The CNRM-CM5.1 global climate model: description
 413 and basic evaluation. *Climate Dynamics*, *40*(9-10), 2091–2121.
- 414 Wei, J., & Wang, H. (2004). A possible role of solar radiation and ocean in the
 415 mid-Holocene East Asian monsoon climate. *Advances in Atmospheric Sciences*,
 416 *21*(1), 1–12.
- 417 Wu, T., Li, W., Ji, J., Xin, X., Li, L., Wang, Z., ... others (2013). Global carbon
 418 budgets simulated by the Beijing Climate Center Climate System Model for
 419 the last century. *Journal of Geophysical Research: Atmospheres*, *118*(10),
 420 4326–4347.
- 421 Yianilos, P. N. (1993). Data structures and algorithms for nearest neighbor search in
 422 general metric spaces. In *Soda* (Vol. 93, pp. 311–21).
- 423 You, Q.-L., Ren, G.-Y., Zhang, Y.-Q., Ren, Y.-Y., Sun, X.-B., Zhan, Y.-J., ... Kr-
 424 ishnan, R. (2017). An overview of studies of observed climate change in the

425 Hindu Kush Himalayan (HKH) region. *Advances in Climate Change Research*,
426 8(3), 141–147.